

# Millimeter observations of Planetary Nebulae: a contribution to the Planck pre-launch catalogue

G. Umana<sup>1</sup>, P. Leto<sup>1,2</sup>, C. Trigilio<sup>1</sup>, C. S. Buemi<sup>1</sup>, P. Manzitto<sup>3</sup>, S. Toscano<sup>3</sup>, S. Dolei<sup>3</sup>, L. Cerrigone<sup>3,4</sup>

<sup>1</sup> INAF - Osservatorio Astrofisico di Catania, Via S. Sofia 78, 95123 Catania, Italy

<sup>2</sup> INAF Istituto di Radioastronomia, Sezione di Noto, C.P. 161, Noto(SR), Italy

<sup>3</sup> Università di Catania, Dipartimento di Fisica e Astronomia, Via S. Sofia 78 , 95123 Catania, Italy

<sup>4</sup> Harvard-Smithsonian Center for Astrophysics, Cambridge, MA 02138, USA

Received; Accepted

## ABSTRACT

*Aims.* We present new millimetre 43 GHz observations of a sample of radio-bright Planetary Nebulae. Such observations were carried out to have a good determination of the high-frequency radio spectra of the sample in order to evaluate, together with far-IR measurements (IRAS), the fluxes emitted by the selected source in the millimetre and sub-millimetre band. This spectral range, even very important to constraint the physics of circumstellar environment, is still far to be completely exploited.

*Methods.* To estimate the millimetre and sub-millimetre fluxes, we extrapolated and summed together the ionized gas (free-free radio emission) and dust (thermal emission) contributions at this frequency range. By comparison of the derived flux densities to the foreseen sensitivity we investigate the possible detection of such source for all the channels of the forthcoming ESA's PLANCK mission.

*Results.* We conclude that almost 80% of our sample will be detected by PLANCK, with the higher detection rate in the higher frequency channels, where there is a good combination of brighter intrinsic flux from the sources and reduced extended Galactic foregrounds contamination despite a worst instrumental sensitivity. From the new 43 GHz, combined with single-dish 5 GHz observations from the literature, we derive radio spectral indexes, which are consistent with optically thin free-free nebula. This result indicates that the high frequency radio spectrum of our sample sources is dominated by thermal free-free and other emission, if present, are negligible.

**Key words.** stars: Planetary Nebulae – Planetary Nebulae: general radio continuum: stars

## 1. Introduction

The PLANCK ESA mission will provide us with nearly full sky maps over a wide range of frequencies, from 30 to 900 GHz. Therefore, even if designed for cosmological studies, the mission will have profound impact on fundamental Physics and Galactic and extragalactic astrophysics. Planck will be sensitive to the millimetre emission from dusty envelopes of stars and we expect the dusty circumstellar envelopes, that characterize the latest stages of stellar evolution, to be source of relevant foreground contamination. When a low or intermediate mass star is approaching the end of its evolution, it goes through a period of heavy mass-loss known as Asymptotic Giant Branch (AGB) phase. The ejected envelopes are partially condensed in dust grains and completely obscure the central star. Immediately after the AGB evolutionary phase, the mass-loss stops and the stars may become optically visible as the dusty shells disperse (Proto Planetary Nebula, PPN phase).

Eventually, once it reaches a temperature of  $2 - 3 \times 10^4$  K, the central star starts to ionize the AGB shell and a Planetary Nebula will form. Dusty envelopes re-radiate the absorbed stellar light showing a clear signature in the far-infrared spectrum, i.e. an IR excess with peculiar IRAS colours. In addition to that, PNe show a radio continuum due to free-free emission from the fraction of the CSE ionized by the central star.

From a feasibility study, Umana et al. (2006) concluded that a sizable ( $\approx 300$ ) sample of AGB and post-AGB stars would be detected during the mission and derived estimates for the expected flux densities at various Planck channels. However, the simulations carried out by Umana et al. (2006), on a sub-sample of PNe rely only on NVSS fluxes, obtained at 1.4 GHz, extrapolated to the Planck frequencies. This leads to underestimate the contribution due to free-free as, at this frequency, PNe are often optically thick (Siodmiank & Tylenka 2001, Luo et al. 2005).

PNe are among the brightest Galactic radio sources. Some of them could also reach a flux density of Jy level. More than 800 have been detected at least at one frequency and for 200

**Table 1.** The selected sample

IAU Name PN G	Other Name	R.A. (J2000) [ h m s]	Dec. (J2000) [ ° ' '' ]	IAU Name PN G	Other Name	R.A. (J2000) [ h m s]	Dec. (J2000) [ ° ' '' ]
000.3 + 12.2	IC 4634	17 01 33.6	-21 49 33.1	093.4 + 05.4	NGC 7008	21 00 32.7	+54 32 39.4
002.4 + 05.8	NGC 6369	17 29 20.5	-23 45 35.0	093.5 + 01.4	PN M 1-78	21 20 44.8	+51 53 27.5
003.1 + 02.9	PN Hb 4	17 41 52.8	-24 42 09.3	096.4 + 29.9	NGC 6543	17 58 33.4	+66 37 58.8
006.7 - 02.2	PN M 1-41	18 09 30.6	-24 12 28.7	097.5 + 03.1	PN A66 77	21 32 10.2	+55 52 43.2
007.2 + 01.8	PN HB 6	17 55 07.0	-21 44 41.0	106.5 - 17.6	NGC 7662	23 25 53.9	+42 32 04.7
008.0 + 03.9	NGC 6445	17 49 15.0	-20 00 33.7	107.8 + 02.3	NGC 7354	22 40 19.9	+61 17 08.0
008.3 - 01.1	PN M 1-40	18 08 26.0	-22 16 53.4	120.0 + 09.8	NGC 40	00 13 01.0	+72 31 19.6
009.4 - 05.0	NGC 6629	18 25 42.5	-23 12 11.3	130.9 - 10.5	NGC 650-51	01 42 19.7	+51 34 31.7
009.6 + 14.8	NGC 6309	17 14 04.3	-12 54 37.2	138.8 + 02.8	IC 289	03 10 19.3	+61 19 00.4
010.1 + 00.7	NGC 6537	18 05 13.1	-19 50 34.4	144.5 + 06.5	NGC 1501	04 06 59.3	+60 55 14.7
010.8 - 01.8	NGC 6578	18 16 16.5	-20 27 03.4	165.5 - 15.2	NGC 1514	04 09 16.9	+30 46 32.0
011.7 - 00.6	NGC 6567	18 13 45.2	-19 04 35.6	166.1 + 10.4	IC 2149	05 56 23.9	+46 06 17.4
020.9 - 01.1	PN M 1-51	18 33 29.0	-11 07 26.3	173.7 + 02.7	PP 40	05 40 52.7	+35 42 18.6
025.8 - 17.9	NGC 6818	19 43 57.8	-14 09 11.8	194.2 + 02.5	J 900	06 25 57.3	+17 47 27.6
027.7 + 00.7	PN M 2-45	18 39 21.9	-04 19 52.6	197.8 + 17.3	NGC 2392	07 29 10.8	+20 54 41.6
033.8 - 02.6	NGC 6741	19 02 37.0	-00 26 57.2	206.4 - 40.5	NGC 1535	04 14 15.8	-12 44 22.3
034.6 + 11.8	NGC 6572	18 12 06.3	+06 51 12.4	215.2 - 24.2	IC 418	05 27 28.2	-12 41 50.2
035.1 - 00.7	PN Ap 2-1	18 58 10.5	+01 36 57.5	221.3 - 12.3	IC 2165	06 21 42.8	-12 59 13.9
037.7 - 34.5	NGC 7009	21 04 10.8	-11 21 48.5	234.8 + 02.4	NGC 2440	07 41 55.4	-18 12 30.5
039.8 + 02.1	PN K 3-17	18 56 18.2	+07 07 26.2	254.6 + 00.2	NGC 2579	08 20 54.1	-36 13 00.0
041.8 - 02.9	NGC 6781	19 18 28.1	+06 32 20.0	258.1 - 00.3	Hen 2-9	08 28 28.0	-39 23 39.4
043.1 + 37.7	NGC 6210	16 44 29.5	+23 47 59.9	259.1 + 00.9	Hen 2-11	08 37 08.1	-39 25 04.9
045.7 - 04.5	NGC 6804	19 31 35.1	+09 13 30.2	261.0 + 32.0	NGC 3242	10 24 46.1	-18 38 32.3
050.1 + 03.3	PN M 1-67	19 11 31.1	+16 51 32.0	294.1 + 43.6	NGC 4361	12 24 30.8	-18 47 04.0
054.1 - 12.1	NGC 6891	20 15 08.9	+12 42 15.4	342.1 + 10.8	NGC 6072	16 12 58.4	-36 13 46.6
063.1 + 13.9	NGC 6720	18 53 35.1	+33 01 45.1	349.5 + 01.0	NGC 6302	17 13 44.5	-37 06 11.6
064.7 + 05.0	BD+30 3639	19 34 45.2	+30 30 59.2	352.6 + 00.1	PN H 1-12	17 26 24.3	-35 01 41.8
082.1 + 07.0	NGC 6884	20 10 23.7	+46 27 40.0	352.8 - 00.2	PN H 1-13	17 28 27.7	-35 07 30.4
083.5 + 12.7	NGC 6826	19 44 48.2	+50 31 31.3	358.5 + 02.6	PN HDW 8	17 31 47.3	-28 42 03.5
086.5 - 08.8	PN Hu 1-2	21 33 08.2	+39 38 08.3	358.5 + 05.4	PN M 3-39	17 21 11.5	-27 11 37.0
089.0 + 00.3	NGC 7026	21 06 18.7	+47 51 07.5	359.3 - 00.9	Pn HB 5	17 47 56.3	-29 59 40.6

morphological and spectral information (between 1.4 and 22 GHz) were obtained. Most of the higher frequency (22 GHz) data were obtained with interferometers (i.e. VLA) while very little single-dish, high frequency measurements are available.

In this paper we present new 43 GHz, single-dish observations by using the 32 m INAF-IRA Radiotelescope at Noto of a sample of PNe, which are potential foregrounds for PLANCK. The main goal of this project is to obtain reliable estimates of flux density expected at PLANCK channels, by building and modeling their spectral energy distribution (SED). This in turn will contribute to the compilation of the PLANCK pre-launch catalogue. We stress here that 43 GHz is one of the observing channels of the forthcoming PLANCK mission. Therefore, at this frequency band, we would obtain a direct measurement of the expected flux and not an extrapolation.

As added value, the present work provides the first sizeable dataset of 43 GHz measurements of PNe, that constitute strong constraints to the observed SEDs in the very important spectral region where free-free emission and thermal dust emission may overlap. While interferometric high frequency observations provide us with detailed morphological informa-

tion they quite often fail to entirely recover the extended emission. This eventually leads to underestimate the total radio flux density. This problem is overcome by single-dish observations. Assessing the SEDs in the radio-millimetre spectral range is a crucial step for the study of the physics of dusty envelopes around PN. A correct evaluation of the free-free contribution, up to millimetre range, when combined with information provide by far-IR observations, would allow to determine the presence of an excess due to the presence of a cold dust component/s (Gee et al. 1984; Hoare et al. 1992; Kemper et al. 2002) or of alternative emission mechanisms (Casassus et al. 2007). Since PNe and their progenitors are believed to be among the major sources of recycled interstellar matter, determining the properties of the dust ejected in the ISM is very important to the study of the Galaxy evolution in general.

## 2. The 43 Ghz Noto Survey

### 2.1. Sample Selection

Our sample has been selected mainly from Condon & Kaplan (1998), who performed a cross-correlation between the

**Table 2.** Results

IAU Name PN G	$S_{43\text{ GHz}}$ [mJy]	$\sigma_{43\text{ GHz}}$ [mJy]	$\theta_{1.4\text{ GHz}}$ [arcsec]	Ref.*	$S_{c\ 43\text{ GHz}}$ [mJy]	IAU Name PN G	$S_{43\text{ GHz}}$ [mJy]	$\sigma_{43\text{ GHz}}$ [mJy]	$\theta_{1.4\text{ GHz}}$ [arcsec]	Ref.*	$S_{c\ 43\text{ GHz}}$ [mJy]
000.3 + 12.2	< 180	60	10.0	C H		093.4 + 05.4	< 240	80	49.2	A E	
002.4 + 05.8	1330	110	20.7	C H	1530	093.5 + 01.4	560	35	14.6	A E	600
003.1 + 02.9	100	20	11.6	C H	105	096.4 + 29.9	400	70	11.9	A E	420
006.7 - 02.2	300	90	21.0		345	097.5 + 03.1	230	25	33.4	A E	320
007.2 + 01.8	310	50	10.6	C H	320	106.5 - 17.6	610	40	12.0	A E	640
008.0 + 03.9	180	20	34.6	C G	250	107.8 + 02.3	280	25	16.4	A E	305
008.3 - 01.1	90	20	9.9	C H	95	120.0 + 09.8	420	70	27.6	A E	530
009.4 - 05.0	130	30	12.8	C H	135	130.9 - 10.5	140	40	59.3	A E	310
009.6 + 14.8	270	60	14.3	C H	290	138.8 + 02.8	< 150	50	23.1	A E	
010.1 + 00.7	400	60	11.8	C F H	420	144.5 + 06.5	215	30	34.9	A E	305
010.8 - 01.8	130	20	11.9	C H	135	165.5 - 15.2	220	30	94.4	A E	890
011.7 - 00.6	< 150	50	8.7	C H		166.1 + 10.4	100	30	9.1	A E	105
020.9 - 01.1	420	90	13.5	C	445	173.7 + 02.7	260	20	11.5	E	270
025.8 - 17.9	270	30	14.7	C H	290	194.2 + 02.5	90	20	0.0	A E H	90
027.7 + 00.7	110	20	0.0	B G	110	197.8 + 17.3	240	50	22.2	A E H	280
033.8 - 02.6	290	50	14.7	E H	310	206.4 - 40.5	160	20	20.6	C H	180
034.6 + 11.8	1220	100	11.9	A E H	1280	215.2 - 24.2	1100	100	0.0	C H	1100
035.1 - 00.7	170	20	13.0	A E	180	221.3 - 12.3	350	50	11.0	C H	365
037.7 - 34.5	375	40	14.9	C H	400	234.8 + 02.4	350	20	16.5	C H	380
039.8 + 02.1	240	20	0.0	A E	240	254.6 + 00.2	1770	290	41.2	F	2800
041.8 - 02.9	230	20	78.4	A E H	715	258.1 - 00.3	180	40	4.5	D H	181
043.1 + 37.7	230	30	10.8	A E H	240	259.1 + 00.9	270	60	42.2	D	435
045.7 - 04.5	140	20	25.4	A B E H	170	261.0 + 32.0	290	30	19.5	C H	330
050.1 + 03.3	140	30	41.4	A E H	220	294.1 + 43.6	130	20	47.3	C H	230
054.1 - 12.1	130	40	8.9	A E H	135	342.1 + 10.8	< 210	70	32.9	H	
063.1 + 13.9	255	75	48.2	A E	460	349.5 + 01.0	2150	220	14.8	D F H	2310
064.7 + 05.0	565	20	10.5	A E	585	352.6 + 00.1	815	125	10.3	F	845
082.1 + 07.0	250	50	11.0	A E	260	352.8 - 00.2	420	50	14.8	F	450
083.5 + 12.7	320	40	15.9	A E	350	358.5 + 02.6	< 120	40	21.1	C G	
086.5 - 08.8	< 120	40	10.4	A E		358.5 + 05.4	380	40	0.0	C G	380
089.0 + 00.3	220	30	11.9	A E	230	359.3 - 00.9	290	70	0.0	F H	290

\* References for 5 GHz measurements: A) Gregory et al. (1996); B) Griffith et al. (1995); C) Griffith et al. (1994); D) Wright et al. (1994); E) Becker et al. (1991); F) Haynes et al. (1979); G) Milne (1979); H) Milne (1975)

Strasbourg-ESO Catalogue of Galactic Planetary Nebulae (Cat. <V/84>, Acker et al. 1992) and the 1.4 GHz NRAO VLA Sky Survey (NVSS). Among these sources we selected only those whose flux densities at 1.4 GHz (NVSS) is higher than 100 mJy, for a total of 64 PNe. In the conservative hypothesis of optically thin nebula at 1.4 GHz, a cut-off at 100 mJy guarantees a 43 GHz flux density easily detectable with the Noto Radiotelescope. This estimated 43 GHz flux density will be a lower limit in the case of optically thick nebula at 1.4 GHz. We also considered Condon et al. (1999) who selected infrared PNs in NVSS by cross-correlation between NVSS and a sample from IRAS PSC on the basis of infrared colours characteristic of PNe. Only 3 over the 122 of infrared PNs candidate have  $S_{1.4\text{ GHz}} \geq 100$  mJy, yielding to a *final* sample of 67 objects.

To avoid problems due to possible contamination in the Noto beam (HPBW= 54''), for each source of the sample, we have extract from NVSS a 25' × 25' field, centred at the position of the target. Sources that show a very extended ( $\geq 2'$ ) emission or that are located in very high confusion region have been rejected. This reduces our sample to 62 objects. The list

of the selected targets, with names and positions, is reported in Table 1.

## 2.2. Observations and Results

In the last few years the INAF-IRA 32m Noto radiotelescope has been subjected to a series of structural improvements which have increased remarkably its potential capabilities as single dish instrument. In particular, the installation of an active surface allows to operate with good performances at high frequencies.

The observations reported in this paper were carried out in different epochs, between 2005 and 2006. The 43 GHz superheterodyne receiver is cooled double polarization receiver, with typical zenith system temperature ( $T_{\text{sys}}$ ), in both channels, of the order of 80 – 100 K, depending on the weather conditions. The gain ranges from 0.05 to 0.1 K/Jy (Leto et al. 2006), depending on elevation, and this determines a zenith System Equivalent Flux Density (SEFD) of 1600 – 2000 Jy. The observations were performed with a 400 MHz instantaneous band.

All the sources of our sample were observed with the on the fly (OTF) scan technique, which consists in driving the beam of the telescope across the source in RA direction. The typical scan duration was of the order of 20 secs, short enough to remain close enough to the white noise regime of the radiometer. In order to achieve a good signal to noise ratio, each source was observed many times, for a total integration time of 30 minutes. Multiple OTF scans were then added together reaching a typical rms of 2 – 3 mK.

Daily gain curves were obtained and the flux scale was fixed by using NGC7027 as primary calibrator and 3C286 as secondary calibrator. The adopted flux densities for NGC7027 and 3C286 are respectively: 5.07 and 1.86 Jy. The assumed flux densities are those reported by Ott et al. (1994); in the case of NGC7027 the measure has been corrected for the observed decreasing of 0.15 percent/year as reported by Perley et al. (2006).

We detected 55 out of the 62 observed objects, with a 89 % detection rate. Results of such observations are reported in Table 2, where the 43 GHz measured flux density, or its  $3\sigma$  upper limit, is listed. In the 4<sup>th</sup> and 10<sup>th</sup> columns of the same table we report the angular size at 1.4 GHz of each source ( $\theta_{1.4 \text{ GHz}}$ ), as derived from the analysis of the relative NVSS map, which has an angular resolution of 45". The source angular size has been derived as the geometrical mean of the minor and major axes obtained by fitting a two dimensional Gaussian at the source position in the map of the brightness distribution, by using the task JMFIT of the NRAO Astronomical Image Processing System (AIPS).

To take into account for possible partial resolution of the source by the Noto beam, assuming that the source size at 43 GHz is the same as measured at 1.4 GHz, we corrected the measured flux density as

$$S_{c \text{ 43 GHz}} = S_{43 \text{ GHz}} \times \frac{\theta_{\text{Noto}}^2 + \theta_{1.4 \text{ GHz}}^2}{\theta_{\text{Noto}}^2}$$

where  $\theta_{1.4 \text{ GHz}}$  and  $\theta_{\text{Noto}}$  are the width of the source at 1.4 GHz (reported in Table 2) and the width of the Noto radiotelescope beam (HPBW=54") respectively. Sources having angular size greater than 25", comparable to the 43 GHz Noto beam (HPBW), have flux corrections significantly larger than the rms associated to the flux density. This means that they cannot be regarded as point-like. The resulting fluxes  $S_{c \text{ 43 GHz}}$  are listed in Table 2.

### 3. The SEDs

#### 3.1. The free-free contribution

As a first step in our analysis, we derived the spectral index  $\alpha$ , ( $S_\nu \propto \nu^\alpha$ ), by combining the fluxes measured at 43 GHz with the 5 GHz single dish measurements available from literature. In order to prevent any error due to resolving out some of the flux density, we considered only the objects that have angular size, at 1.4 GHz ( $\theta_{1.4 \text{ GHz}}$ ), lower than 25". This reduces our sample detected sources to 42 PNe that can be, quite confidentially, considered point-like with respect to the telescope beam at the observational frequency. Literature 5 GHz data are

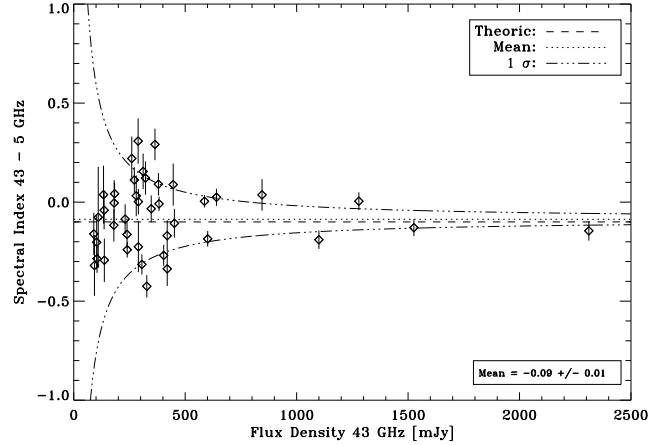


**Fig. 1.** Calculated spectral index as function of flux at 43 GHz. As expected major dispersion is evident at lower fluxes

available only for 41 targets. The 5 GHz single dish measurements are from surveys performed by NRAO Green Bank 91 cm telescope, with a beamwidth (HPBW)  $\approx 3.5'$  (Gregory et al. 1996, Becker et al. 1991) and Parkers 64 m telescope with a beamwidth  $\approx 4.5'$  (Griffith et al. 1995, Griffith et al. 1994, Wright et al. 1994, Haynes et al. 1979, Milne 1979 and Milne & Aller 1975), as indicated in Table 2. For the sources observed in more than one survey, we used the average of the fluxes from the different measurements.

The spectral indices  $\alpha$ , calculated between the two frequencies, are shown in Fig. 1 as a function of the flux density at 43 GHz. Since its accuracy depends on the value of the measured flux densities and associated uncertainties, we computed the expected  $1\sigma$  as a function of the flux density, assuming a typical rms, associated to the 43 GHz and 5 GHz measurements, of  $\sigma_{43\text{GHz}} \approx 50 \text{ mJy}$  and a  $\sigma_{5\text{GHz}} \approx 35 \text{ mJy}$ , respectively. The  $\pm 1\sigma$  uncertainty values around the mean value  $\alpha = -0.09$  are shown in Fig. 1 as dot-dashed lines. For about 70% of the sources we get a spectral index inside the uncertainty lines, showing that it is statistically consistent with the value  $\alpha = -0.1$ , typical for an optically thin free-free emission. We may conclude that for our sample, at least up to 43 GHz, the SED is dominated by the free-free emission and other contributions, if present, are negligible.

#### 3.2. The dust contribution

PNs are usually surrounded by a dusty envelope which is the remnant of the precursor's wind. Dust thermally re-radiates the UV radiation of the central star determining an excess that may extend from the far-IR to the radio region. Such a contribution is typically of the order of 40% of the total flux from a PNe (Zhang & Kwok 1991), being more important in young PNe, since, in more evolved PNe, the circumstellar material has already dispersed. We built the dust component of our sample of PNe by using IRAS measurements.

The IRAS data have been fitted by assuming that the dust emits as a blackbody modified by the frequency dependent dust

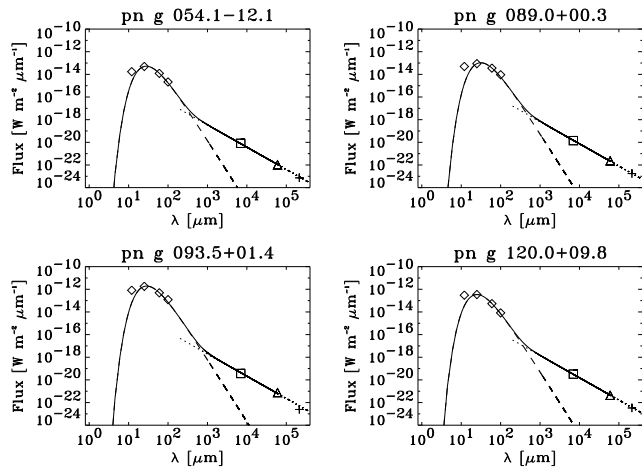


**Fig. 2.** Spectral Energy Distributions of four of our targets. Both ionized gas (dotted line) and thermal dust (dashed line) contributions are shown. Continuous line is the total emission. Diamonds: IRAS data; squares: our measures at 43 GHz ( $7 \times 10^3 \mu\text{m}$ ); triangle: literature measures at 5 GHz ( $6 \times 10^4 \mu\text{m}$ ); cross: NVSS data at 1.4 GHz ( $2 \times 10^5 \mu\text{m}$ )

opacity, that is  $F_\nu \propto \nu^p B_\nu(T_d)$ , where  $B_\nu(T_d)$  is the Planck function for dust temperature  $T_d$ , and  $p$  is the emissivity index. The index  $p$  strongly depends on the mineralogical composition of the grain and on their physical shape. In our calculation, following the results from detailed modelling of dust emission from PNe (Hoare 1990), we assumed, for the slope of the far-IR emissivity law, a typical value of  $p=1.5$ . Because strong contamination by line emission of 12  $\mu\text{m}$  IRAS band (Stasinska & Szczerba 1999) only 25, 60 and 100  $\mu\text{m}$  fluxes have been used in the fitting procedure.

#### 4. Estimates of flux density at Planck channels

The SEDs with both ionized gas and dust contribution, evaluated in Sect. 3.1 and 3.2, were built for all the targets in our sample. In Fig. 2, four of such SEDs are shown as an example. In the SEDs, between radio and far-IR there is a large gap where measurements are missing. New millimetre and sub-millimetre observations are clearly necessary to better characterize and constraint the emission from different components, where the radio flux, from the ionized fraction of the nebula, could be merged to the dust contribution. This gap will be partially filled by the ESA-PLANCK mission, as the satellite is equipped with a Low Frequency Instruments (LFI), operating at 30, 44 and 70 GHz, and a High Frequency Instruments (HFI), operating at 100, 143, 217, 353, 545 and 857 GHz.

In order to evaluate the possibility that PLANCK will actually detect sources in our sample, we should compare, for each observational band, the expected flux from the sources to the foreseen sensitivity. The expected fluxes are derived by summing, at each PLANCK channel, both dust and ionized gas contribution. The first has been obtained by extrapolating the modified blackbody fit (dashed lines in Fig. 2); the latter has been obtained from fitting free-free emission from an optically thin nebula to the 5 GHz ( $6 \times 10^4 \mu\text{m}$ ) and 43 GHz ( $7 \times 10^3 \mu\text{m}$ )

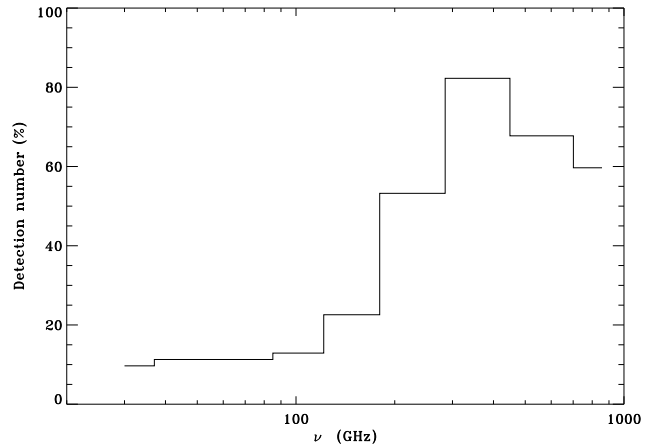


**Fig. 3.** Histogram showing the fraction of planetary nebulae belonging to our sample that can be detected by the Planck satellite

data points and then extrapolating to the Planck channels (dotted line in Fig. 2), the NVSS measures at 1.4 GHz ( $2 \times 10^5 \mu\text{m}$ ) has been also displayed.

Following Umana et al. (2006), the foreseen total sensitivity is assumed to be the sum in quadrature of all the sources of confusion noise, namely: the nominal instrumental Planck sensitivity per resolution element; the Galactic and extragalactic foregrounds confusion noise (Toffolatti et al. 1998); the CMB confusion noise (Bennett et al. 2003). All the considered confusion sources will contribute to a total sensitivity ( $\sigma$ ) ranging from 270 mJy for the 30 GHz channel to 220 mJy for the 857 GHz channel. In Fig. 3 we show the percentage of the objects from our sample that could be detected over the  $3\sigma$  threshold for each channels of the PLANCK instruments. A small number of PNe belonging to our sample will be detected by PLANCK in the radio (LFI channels), while most of our targets will be easily seen by PLANCK in the millimetre and sub-millimetre bands (HFI channels). We may conclude that we foresee an important contribution of the PLANCK mission also to the study of PNe, as it would provide measurements in a very important, but still far to be fully explored, spectral region.

#### 5. Summary

We have presented new 7 mm (43 GHz) observations of a sample of radio-bright PNe, carried out with the INAF-IRA Noto Radiotelescope. Such observations have been used to derive the high-frequency free-free contribution, due to the ionized fraction of the circumstellar envelope. So far, the majority of high frequency radio observations of PNe have been conducted with interferometers, that reveal details of source radio morphology but could, in principle, resolve out some of the extended emission. Our single dish measurements provide an extended database of millimetre observations of PNe, to be used when is necessary to know the overall emission, such as when building a SED. We used our measurements, that trace the free-free contribution, together with IRAS measurements, which trace the thermal dust emission, to build up the observed SED, from

radio to far-IR and by extrapolation, to estimate the expected fluxes in the spectral range between radio and sub-mm, where observational data are missing.

When comparing the expected millimetre-sub-millimetre fluxes with the total foreseen sensitivity of the forthcoming ESA mission PLANCK we estimate that a consistent number of our targets will be easily detected by PLANCK, mostly at higher frequency channels. Therefore, even if designed for cosmological study, PLANCK could also contribute to the PNe science. Results from such kinds of observations, once modelled with appropriate code (i.e. CLOUDY, DUSTY), would provide important constraints on the chemical composition and structure of the CSEs. It would point out the presence of multi-shells, related to multiple mass-loss event suffered from the central object during its previous evolution (AGB), or a contribution of different emission processes, besides free-free and thermal from dust, as recently claimed by Cassassus et al. (2007). Moreover, PLANCK results can be considered as pathfinder for other future instrumentations, with the same frequency coverage, such as ALMA, as they will help in planning more focused experiments aimed to investigate the morphological details of the sources.

*Acknowledgements.* Based on observations with the Noto Telescope operated by INAF-Istituto di Radioastronomia This work has been partially supported by ASI through contract Planck LFI Activity of Phase E2.

## References

- Acker, A., Ochsenbein, F., Stenholm, B., Tyllenda, R., Marcout, J., Schohn, C. 1992, ESOPN, 1, 1
- Becker, R.H., White, R.L., Edwards, A.L. 1991, ApJS, 75, 1
- Bennett, C.L. 2003, ApJS, 148, 1
- Cassassus, S., Nyman, L.A., Dickinson, C., Pearson, T.J. 2007, MNRAS, accepted (arXiv:0708.2385)
- Condon, J.J., Kaplan, D.L. 1998, ApJS, 117, 361
- Condon, J.J., Kaplan, D.L., Terzian, Y. 1999, ApJS, 123, 219
- Gee, G., Emerson, J.P., Ade, P.A.R., Robson, E.I., Nolt, I.G. 1984, MNRAS, 208, 517
- Gregory, P.C., Scott, W.K., Douglas, K., Condon, J.J. 1996, ApJS, 103, 427
- Griffith, M.R., Wright, A.E., Burke, B.F., Ekers, R.D. 1994, ApJS, 90, 179
- Griffith, M.R., Wright, A.E., Burke, B.F., Ekers, R.D. 1995, ApJS, 97, 347
- Haynes, R.F., Caswell, J.L., Simons, L.W.J. 1979, AuJPA, 48, 1
- Hoare, M.G. 1990, MNRAS, 244, 193
- Hoare, M.G., Roche, P.F., Clegg, R.E.S. 1992, MNRAS, 258, 257
- Leto, P., Buemi, C. S., Trigilio, C., Umana, G., Toscano, S., Nocita, C. 2006, MSAIS, 10, 87
- Luo, S.G., Condon, J.J., Yin, Q.F. 2005, ApJS, 159, 282
- Kemper, F., Molster, F.J., Jager, C., Waters, L.B.F.M. 2002, A&A, 394, 679
- Milne, D.K., Aller, L.H. 1975, A&A, 38, 183
- Milne, D.K. 1979, A&AS, 36, 227
- Ott, M., Witzel, A., Quirrenbach, A., Krichbaum, T.P., Standke, K.J., Schalinski, C.J., Hummel, C.A. 1994, A&A, 284, 3310
- Perley, R.A., Zijlstra, A., van Hoof, P. 2006, AAS, 209, 9202
- Siodmiak, N., Tyllenda, R. 2001, A&A, 373, 1032
- Szasinska, G., Szczerba, R. 1999, A&A, 352, 297
- Toffolatti, L., Argueso Gomez, F., de Zotti, G., Mazzei, P., Franceschini, A., Danese, L., Burigana, C. 1998, MNRAS, 297, 117
- Umana, G., Burigana, C., Trigilio, C. 2006, MSAIS, 9, 279.
- Wright, A.E., Griffith, M.R., Burke, B.F., Ekers, R.D. 1994, ApJS, 91, 111
- Zhang, C.Y., Kwok, S. 1991, A&A, 250, 179